Smart Structures and Systems, Vol. 9, No. 6 (2012) 549-563 549
DOI: http://dx.doi.org/10.12989/sss.2012.9.6.549

Analysis and simulation of multi-mode piezoelectric energy harvesters

Ying Zhang* and Binghu Zhu

School of Electrical and Computer Engineering, Georgia Institute of Technology, Atlanta, GA, USA

(Received September 1, 2011, Revised April 5, 2012, Accepted May 22, 2012)

Abstract. Theoretical analysis is performed on a multi-mode energy harvester design with focus on the first two vibration modes. Based on the analysis, a modification is proposed for designing a novel adaptive multi-mode energy harvester. The device comprises a simply supported beam with distributed mass and piezoelectric elements, and an adaptive damper that provides a 180 degree phase shift for the motions of two supports only at the second vibration mode. Theoretical analysis and numerical simulations show that the new design can efficiently scavenge energy at the first two vibration modes. The energy harvesting capability of the multi-mode energy harvester is also compared with that of a cantilever-based energy harvester for single-mode vibration. The results show that the energy harvesting capacity is affected by the damping ratios of different designs. For fixed damping ratio and design dimensions, the multi-mode design has higher energy harvesting capacity than the cantilever-based design.

Keywords: multi-mode design; piezoelectric energy harvester; vibration; adaptive damper; phase shift

1. Introduction

Ambient energy harvesting has been investigated to extend the lifetime of wireless sensor networks for a broad range of applications. Potential ambient energy sources include mechanical vibration (Roundy *et al*. 2003, Glynne-Jones *et al*. 2004, Mitcheson *et al.* 2004, Shu and Lien 2006, Tiwari *et al.* 2008), light (Yu *et al.* 1995, Yu and Heeger 1995, Bach *et al.* 1998, Neugebauer *et al.* 2000, Paradiso and Starner 2005, MacNeil and Sargent 2006), thermal gradient (Venkatasubramanian et al. 2001, Snyder *et al*. 2003), strain (Lysne and Percival 1975, Xu *et al.* 1997, Engel *et al.* 2000, Keawboonchuay and Engel 2003, Gao *et al.* 2004) and wind (Burton *et al.* 2001, Munteanu et al. 2006). The most mature and commercially available method to scavenge energy is based on solar cells. While solar cells are attractive for some outdoor applications, they are not useful for sensors that are not accessible to the direct sunlight and the harvested power is too low on a cloudy day. Mechanical vibrations, existing almost everywhere, have been investigated as a promising energy source for wireless sensors in some applications, such as machine condition monitoring and indoor environmental monitoring (Roundy *et al.* 2003, Roundy and Wright 2004, James *et al*. 2004, Leland *et al.* 2004, Roundy 2005). Energy harvesting devices pick up vibrations on a vibrating source, and then convert vibration energy to electrical energy using piezoelectric materials (Shu and Lien 2006, Sodano *et al*. 2004, Anton and Sodano 2007),

*Corresponding author, Assistant Professor, E-mail: yzhang@gatech.edu

electromagnetic induction (Glynne-Jones *et al*. 2004, James *et al*. 2004, Cullen *et al.* 1997, El-hami *et al*. 2001, Yang *et al*. 2009), or electrostatic methods (Sterken *et al.* 2003, Yen and Lang 2006). Since electrostatic transducers require a separate voltage source (such as a battery) to begin the conversion cycle and electromagnetic transducers typically output *AC* voltages well below one volt in magnitude (extra electronics might be needed to boost the output voltage) (Shahruz 2006), piezoelectric generators are of primary interest.

Most piezoelectric vibration energy harvesters studied so far are based on simple cantilever-based design with resonant frequency matching the environmental resonant frequency (Sodano *et al*. 2004, Anton and Sodano 2007). The simple cantilever-based energy harvester is efficient only when its resonant frequency is tuned to match the environmental resonant frequency. If the resonant frequency is mismatched, the energy conversion efficiency drops dramatically. This type of vibration energy harvester will fail to collect sufficient power for wireless sensors if used in an environment with vibration frequencies far away from the resonant frequency of the device.

Piezoelectric vibration energy harvesters with an array of cantilevers have been investigated to provide broadband energy harvesters (Shahruz 2006, 2008, Qi *et al*. 2010). The array of cantilevers had a band of closely spaced mechanical resonance peaks, which provided a wide band response for the device. Of course, if the resonant peaks of all cantilever-mass systems are designed to be far away from each other and each cantilever has piezoelectric materials mounted upon it, the design can also provide a multi-mode energy harvester that scavenges energy at different frequencies. However, the device efficiency is low since only one cantilever is vibrating and generating electrical energy at a fixed vibration frequency. Leland and Wright (2006) investigated an energy harvester device with a simply supported piezoelectric bimorph as its active element and a proof mass mounted at the bimorph's center. They demonstrated that a variable compressive axial preload applied to the bimorph can adjust the resonance frequency of the device. Morris *et al*. (2008) also used a mechanism that adjusts pre-tensions of piezoelectric sheets in an extensional mode resonator to tune the frequency of the device. Although these devices have tunable frequencies, it still can only work efficiently at one frequency once deployed. Some recent research attempted to achieve vibration energy harvesting at multiple frequencies through modifying cantilever-based design either by segmenting the cantilever beam (Lee *et al*. 2009) or by adding a dynamic magnifier to the harvesting beam (Zhou *et al.* 2012).

This paper presents preliminary work in the development of novel multi-mode energy harvesters with distributed stiffness and mass and has multiple resonant frequencies that can be designed to match the multiple environmental vibration modes. Both analytical and numerical simulation approaches are used to investigate the feasibility of such multi-mode energy harvester using a design with two interested resonant modes as an example. The results show an adaptive multi-mode energy harvester has potential to efficiently scavenge vibration energy at two vibration modes. Even for single vibration mode, the new design may have advantages over the cantilever-based design in terms of energy harvesting capacity.

2. Analysis of the single-mode energy harvester

A piezoelectric vibration energy harvester (Fig. 1(a)) may be modeled as a mass-spring-damper-piezo structure (Fig. 1(b)) (Ottman *et al*. 2002, Richard *et al.* 2004, Lefeuvre *et al.* 2005). The dynamic equations governing such system are given by (Lefeuvre *et al.* 2005).

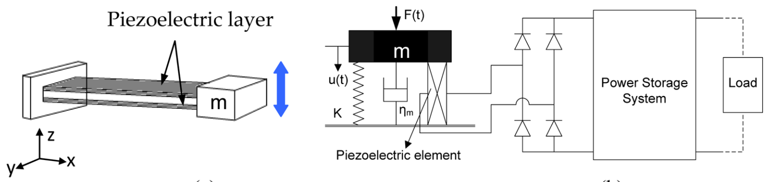

(a) (b)

Fig. 1 (a) A common piezoelectric vibration energy harvester and (b) equivalent model for a piezoelectric vibration energy harvester with standard energy harvesting circuit

$$F = m\ddot{u} + K_e u + \alpha V + C\dot{u} \tag{1}$$

$$\int F\dot{u}dt = \frac{1}{2}m\dot{u} + \frac{1}{2}K_e u^2 + \int C\dot{u}dt + \int \alpha V\dot{u}dt \tag{2}$$

$$\int \alpha V\dot{u}dt = \frac{1}{2}C_0 V^2 + \int VI_C dt \tag{3}$$

where m is the mass of the vibrating block shown in Fig. 1, u is the relative displacement of the mass m with respect to the base, K_e is the equivalent stiffness of the structure, α is the force factor which also represents the measure of the conversion from mechanical energy to electric energy, C is the damping coefficient, C_0 is the clamped capacitance of the piezoelectric element, I_C and V are the outgoing current and the voltage on the piezoelectric element. F is the effective force applied to the mass. If the motion of the base is harmonic of the form $u_b = B\sin(\omega t)$, where B is the amplitude of the base motion, the equivalent load applied to the mass is $F = -m\ddot{u}_b = mB\omega^2 sin(\omega t)$ if resonance occurs.

Considering a load resistor, R, connected directly to the output of the rectifier of the harvester, the voltage on the piezoelectric element can be expressed in the frequency domain as a function of the displacement (Lesieutre *et al*. 2004).

$$\tilde{V} = \frac{\alpha R}{1 + jRC_0\omega} j\omega\tilde{u} \tag{4}$$

where ω is the angular velocity of F.

The frequency domain representation of (1) are given by

$$\tilde{F} = \left(jm\omega + \frac{1}{j\omega}K_e + C + \frac{\alpha^2 R}{jRC_0\omega + 1}\right) j\omega\tilde{u} \tag{5}$$

It follows from the vibration theory that the resonance occurs when ω is close to the resonance frequency of the structure ω_n, and in this case the phase of $\tilde{F}$ always takes $\pi/2$ phase lead compared to $\tilde{u}$. This gives

$$0 = -m\omega_n^2 + K_e + \frac{\alpha^2 R^2 C_0 \omega_n^2}{(RC_0\omega_n)^2 + 1} \tag{6}$$

$$\tilde{F}_{res} = \left(C + \frac{\alpha^2 R}{(RC_0\omega_n)^2 + 1}\right) j\omega_n\tilde{u} \tag{7}$$

from which ω_n is found to be

$$\omega_n = \left[\frac{(-m + K_e R^2 C_0^2 + \alpha^2 R^2 C_0) + \sqrt{(-m + K_e R^2 C_0^2 + \alpha^2 R^2 C_0)^2 + 4K_e m R^2 C_0^2}}{2mR^2 C_0^2} \right]^{\frac{1}{2}} \tag{8}$$

For weakly electromechanically coupled structure, the variable α is close to zero, which leads to simplified expression of ω_n.

$$\omega_n \approx \sqrt{\frac{K_e}{m}} = \sqrt{\frac{3EI}{mL^3}} = 1.732\sqrt{\frac{EI}{mL^3}} \tag{9}$$

Where E is the elastic modulus of the beam material, I is the area moment of inertia of the beam cross-section, and L is the length of the cantilever beam. Note that an assumption we make here is that the structure is with low viscous losses, namely, the damping coefficient C is small. For this reason, we are justified to approximate the resonance frequency ω_r with the natural frequency ω_n.

The harvested power can be expressed as

$$P = \frac{|V|^2}{2R} = \frac{R\alpha^2}{1+(RC_0\omega_n)^2}\frac{\omega_n^2 u_m^2}{2} \tag{10}$$

where u_m is the displacement amplitude.

A maximum $P_{\max}$ is reached when an optimal load R_{opt} is set, namely

$$R_{opt} = \frac{1}{C_0\omega_n} \tag{11}$$

$$P_{\max} = \frac{\alpha^2 \omega_n u_m^2}{4C_0} \tag{12}$$

The force factor, α, is the coupling factor between the force directly applied to the piezoelectric material and the outgoing voltage (Eq. (13)). Its value depends on material properties and dimensions of the piezoelectric material.

$$F_p = K_{PE} u_P + \alpha V \tag{13}$$

Where F_p is the force directly applied to the piezoelectric material, K_{PE} and u_p are the stiffness and the displacement of the piezoelectric material. V is the outgoing voltage on the piezoelectric material.

The overall coupling factor between the external force and the outgoing voltage will differ from that of the underlying materials. It is more convenient to relate the force factor to the external force F in order to compare energy conversion efficiency of different designs. For the design in Fig. 1, thin piezoelectric layers are attached on the top and bottom of a metal layer that behaves like a spring. External force is applied to the mass attached to the spring. The force directly applied to the piezoelectric material is proportional to the surface axial stress at the location. For the comparison purpose, it is appropriate to assume that the force factor α is proportional to the average axial stress $\bar{\sigma}$, where $\bar{\sigma} = \frac{\int_0^L |\sigma(x)| dx}{L}$, namely

$$\alpha = \gamma \frac{\int_0^L |\sigma(x)| dx}{L} \tag{14}$$

Positive constant γ depends on the physical property of the beam and the piezoelectric parameter.
Then for the cantilever vibration energy harvester

$$\sigma(x) = \frac{M(x)\frac{d}{2}}{I} \tag{15}$$

where d is the thickness of the beam and torque M is given by

$$M = F_I\ (L - x) \tag{16}$$

Where x is the distance from the support, and F_I is the inertial force applied to the mass, which can be calculated from

$$F_I = K_e u \tag{17}$$

Plugging Eq. (15) into Eq. (14) gives

$$\alpha = \frac{\gamma d}{2IL}\int_0^L |M(x)|dx = \frac{\gamma d F_I L}{4I} = 0.25\frac{\gamma d\ L K_e u}{I} \tag{18}$$

Plugging Eq. (18) into Eq. (12), we can represent the maximum power in terms of material parameters, design dimensions, and the displacement amplitude of the mass. For weakly electromechanically coupled structure, the mass displacement at resonance can be solved from Eq. (1).

$$u = \frac{F_m}{K_e} R_{dn}\, sin(\omega_n t + \varphi) = \frac{mB\omega_n^2}{K_e} R_{dn}\, sin(\omega_n t + \varphi) = \frac{mB\omega_n^2}{2K_e\xi_n} sin(\omega_n t + \varphi) \tag{19}$$

Where F_m is the amplitude of the sinusoid external excitation force applied to the mass, φ is the phase shift, R_{dn} is the dynamic magnification factor at resonance, and ξ_n is the damping ratio.

$$R_{dn} = \frac{1}{2\xi_n} \tag{20}$$

$$\xi_n = \frac{C}{2\omega_n m} \tag{21}$$

3. Analysis of a multi-mode energy harvester

The simple cantilever-based energy harvester is efficient only when its resonant frequency is tuned to match the environmental resonant frequency. This type of vibration energy harvester is inefficient if used in environments with multiple dominant modes or with a dominant mode that changes with time. Different design concepts have been proposed to design multi-mode energy harvesters (Shahruz 2006, 2008, Qi *et al.* 2010, Zhang and He 2008). One potential approach is to use distributed mass-spring-damper-piezo structures with multiple modes that are adapted to the environmental resonant frequencies to efficiently harvest vibration energy on these structures (Zhang and He 2008). A simple design example is shown in Fig. 2. The dimensions shown in the figure, which are adjustable for different applications, will be used for the theoretical and numerical analysis in this paper. The piezoelectric layer is not shown in Fig. 2. Based on the vibration modes the harvester is designed to use, distributed piezoelectric layer needs to be applied to the top and bottom of the

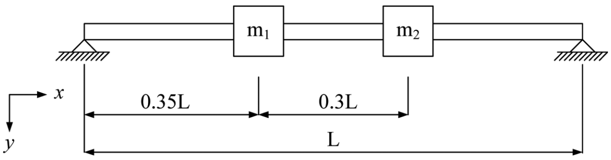

Fig. 2 A simple multi-mode energy harvester with pinned-pinned support

beam to prevent elimination of opposite charges generated from different segments where one segment experiences tension and the other experiences compression. For weakly electromechanically coupled structure, we can first focus on mechanical analysis of the design without piezoelectric layers, and then use Eqs. (14) and (12) to calculate the force factor and the maximum power that can be harvested at different modes.

For the design in Fig. 2, the relative-response equations of motion subjecting to acceleration at the supports can be written as

$$\boldsymbol{M}\ddot{\boldsymbol{u}}+\boldsymbol{K}\boldsymbol{u}+\boldsymbol{C}\dot{\boldsymbol{u}}=\boldsymbol{f} \tag{22}$$

Where $\boldsymbol{M}$, $\boldsymbol{K}$ and $\boldsymbol{C}$ are the mass matrix, the stiffness matrix and the damping matrix respectively. $\boldsymbol{u}$ is the displacement vector of two masses, and $\boldsymbol{f}$ is the effective load vector applied to two masses. For a piezoelectric energy harvester, both supports are often attached to the same base and therefore subjected to the same acceleration. If the motion of the base is harmonic of the form $u_b = B\sin(\omega t)$, the effective load vector is

$$\boldsymbol{f} = -\boldsymbol{M}\{\mathbf{1}\}\ddot{u}_b = \boldsymbol{M}\{\mathbf{1}\}B\omega^2 sin(\omega t) \tag{23}$$

in which $\{\mathbf{1}\}$ represents a column of ones.

To use the analysis results of the single-mode energy harvester in section 2, we transform the coupled Eq. (22) to a system of normal (modal) coordinates due to the orthogonality property of the mode shapes for a linear system.

$$M_i\ddot{Y}_i+K_iY_i+C_i\dot{Y}_i=f_i \tag{24}$$

Where M_i, K_i, C_i, and f_i are the modal-coordinate generalized mass, generalized stiffness, generalized damping coefficient, and generalized load for mode i.

$$\begin{aligned} M_i &= \phi_i^T\boldsymbol{M}\phi_i \\ K_i &= \phi_i^T\boldsymbol{K}\phi_i \\ C_i &= \phi_i^T\boldsymbol{C}\phi_i \\ f_i &= \phi_i^T\boldsymbol{f} \end{aligned} \tag{25}$$

Where ϕ_i is the mode-shape vector for mode i. The required mode shapes ϕ_i $(i = 1,2,...)$ and corresponding frequencies $\hat{\omega}_i$ can be found by solving the eigenvalue problem.

$$[\boldsymbol{K}-\omega^2\boldsymbol{M}]\hat{\boldsymbol{u}} = \boldsymbol{0} \tag{26}$$

Y_i is the modal amplitude. For any modal component $\boldsymbol{u}_i$, the displacements are calculated from

$$\boldsymbol{u}_i = \phi_i Y_i \tag{27}$$

As the support motions tend to excite strongly only the lowest modes of vibration (Clough and Penzien 1993), the energy harvester should be designed to work at the low vibration modes. Our mechanical analysis in this paper will focus on the first two dominant modes and assume two equal masses, i.e., $m_1=m_2$. For a design with two equal masses in Fig. 2, the mass matrix, the stiffness matrix and the damping matrix are

$$\boldsymbol{M} = \begin{bmatrix} m_1 & 0 \\ 0 & m_1 \end{bmatrix} \tag{28}$$

$$\boldsymbol{K} = \begin{bmatrix} K_{11} & K_{12} \\ K_{21} & K_{22} \end{bmatrix} = \frac{EI}{L^3}\begin{bmatrix} 278.4435 & -247.8630 \\ -247.8630 & 278.4435 \end{bmatrix} \tag{29}$$

$$\boldsymbol{C} = \begin{bmatrix} C_{11} & C_{12} \\ C_{21} & C_{22} \end{bmatrix} \tag{30}$$

The first two mode shapes and the corresponding resonant frequencies are

$$\phi_1 = \begin{bmatrix} 1 & 1 \end{bmatrix}^T$$
$$\phi_2 = \begin{bmatrix} 1 & -1 \end{bmatrix}^T \tag{31}$$

$$\hat{\omega}_1 = 5.5300\sqrt{\frac{EI}{m_1L^3}}$$
$$\hat{\omega}_2 = 22.9416\sqrt{\frac{EI}{m_1L^3}} \tag{32}$$

Plugging Eqs. (28)-(30) into Eqs. (24) and (25), we can get two uncoupled dynamic equations for the first two modes. Each equation is similar to the dynamic equation of the single-mode energy harvester. The modal amplitudes of the first two modes can be calculated from Eqs. (19), (23), (25) and (31).

$$Y_1 = \frac{2m_1B\hat{\omega}_1^2}{4(K_{11}+K_{12})\xi_1}sin(\hat{\omega}_1t+\varphi_1)$$
$$Y_2 = \frac{0}{4(K_{11}-K_{12})\xi_2}sin(\hat{\omega}_2t+\varphi_2) \tag{33}$$

where ξ_n is the dampling ratio for the corresponding mode. For the second mode, the generalized load is zero since the mode shape vector is $[1\ -1]^T$ and motions of two bases are same. This results in a modal amplitude of zero for mode 2.

The relative displacements of two mass blocks from the support can be calculated from Eq. (27).

$$\boldsymbol{u}_1 = \phi_1 Y_1 = \left[\frac{m_1 B \hat{\omega}_1^{\ 2}}{2(K_{11}+K_{12})\xi_1} sin(\hat{\omega}_1 t + \varphi_1) \quad \frac{m_1 B \hat{\omega}_1^{\ 2}}{2(K_{11}+K_{12})\xi_1} sin(\hat{\omega}_1 t + \varphi_1) \right]^T$$

$$\boldsymbol{u}_2 = \phi_2 Y_2 = \begin{bmatrix} 0 & 0 \end{bmatrix}^T \tag{34}$$

The equivalent stiffness of the beam at two mass block locations in Fig. 2 is

$$\hat{K}_1 = \frac{3EI}{(0.35L)^2(1.6L)} \tag{35}$$

The inertial force applied to each mass in the first mode is

$$\hat{F}_1 = \hat{K}_1 \hat{u}_1 = \frac{3EI}{(0.35L)^2(1.6L)} \cdot \frac{m_1 B \hat{\omega}_1^{\ 2}}{2(K_{11}+K_{12})\xi_1} sin(\hat{\omega}_1 t + \varphi_1) \tag{36}$$

The torque distribution along the beam is

$$\hat{M}_1 = \begin{cases} \hat{F}_1 x & 0 \le x \le 0.35L \\ 0.35\hat{F}_1 L & 0.35L \le x \le 0.65L \\ \hat{F}_1 (L-x) & 0.65L \le x \le L \end{cases} \tag{37}$$

Using Eqs. (14) and (15), we can calculate the force factor of the design in Fig. 2 in the first mode.

$$\hat{\alpha}_1 = 0.1138 \frac{\gamma d L \hat{F}_1}{I} \tag{38}$$

The second mode of the multi-mode design can not be excited if both supports experience the same motion since the generalized load for the second mode is zero.

Based on the theoretical analysis results, we propose a design adding an adaptive damper to one or both supports so that the motions of two supports have a 180° phase shift close to the second mode, as shown in Fig. 3. Since it is difficult to perform the dynamic analysis for the adaptive multi-mode energy harvester, we use a finite element analysis software, Abaqus, to analyze the dynamic characteristics of the new design.

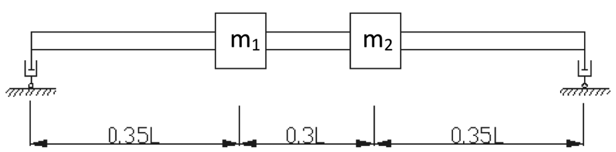

Fig. 3 Adaptive multi-mode energy harvester

Table 1 Material properties and design dimensions of the adaptive multi-mode energy harvester

Length (mm)	Width (mm)	Thickness (mm)	Young's Modulus (MPa)	Poisson's ratio	Mass (kg)	ξ
200	12	1	69e3	0.3	0.100	0.02

4. Simulation of adaptive multi-mode energy harvester

The material properties and design dimensions for the simulation are listed in Table 1.

The first two modes of the adaptive multi-mode energy harvester are shown in Figs. 4 and 5 from modal analysis. The frequency responses of the displacement of each mass are shown in Figs. 6 and 7 with in-phase and out-of-phase base excitations, respectively. For Figs. 4 and 6, the same harmonic motion is applied to both supports with a magnitude of 1 mm. For Figs. 5 and 7, the harmonic motions applied to two supports have the same magnitude (1 mm) and 180 degree phase difference.

In the first mode, the motions of both supports are same. The theoretical analysis in section 3 should apply to the adaptive multi-mode design in the first mode. Numerical simulation verifies that the maximum mass displacement, which is 24.2 mm at 8.2 Hz in the first mode, is very close to the analytical result (25 mm at 8.2 Hz) calculated from Eq. (34). The inertial force (F_{n1}) applied to each mass in the first mode can be calculated from the equivalent stiffness of the beam (K_1) and the displacement of the mass in the first mode (u_{n1}) based on Eqs. (35) and (36).

$$F_{n1} = K_1 u_{n1} = \frac{3EI}{(0.35L)^2(1.6L)} u_{n1} \tag{39}$$

Using Eqs. (14), (15) and (37), the force factor in the first mode is

$$\alpha_{n1} = 0.1138 \frac{\gamma d L F_{n1}}{I} \tag{40}$$

In the second mode, the motions of both supports have a 180 degree phase shift. The maximum

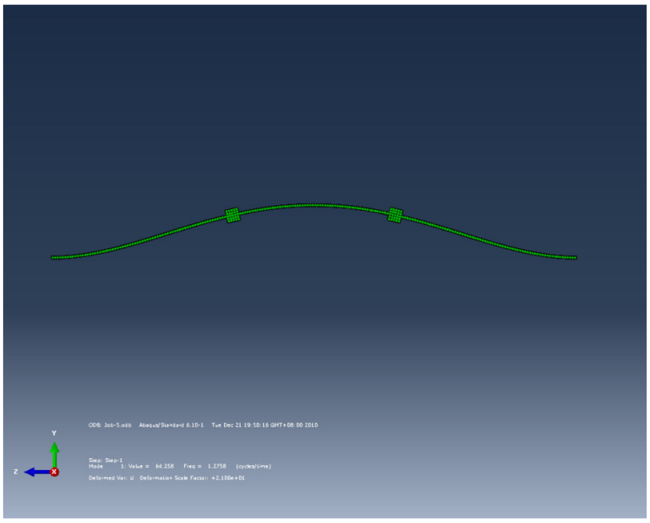

Fig. 4 Modal analysis of the adaptive multi-mode energy harvester in the first mode

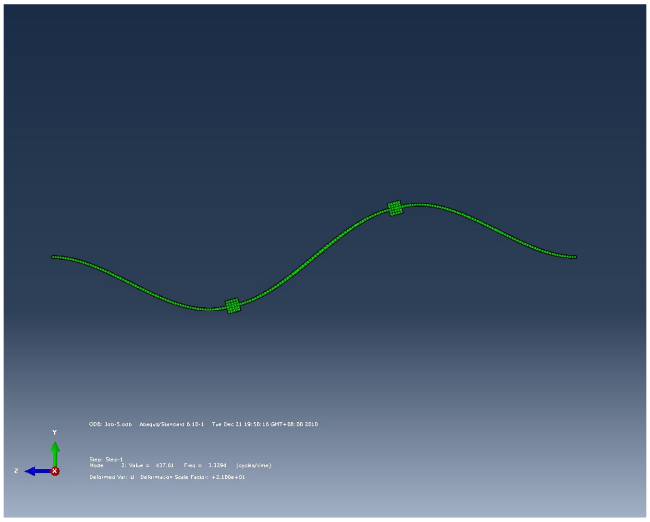

Fig. 5 Modal analysis of the adaptive multi-mode energy harvester in the second mode

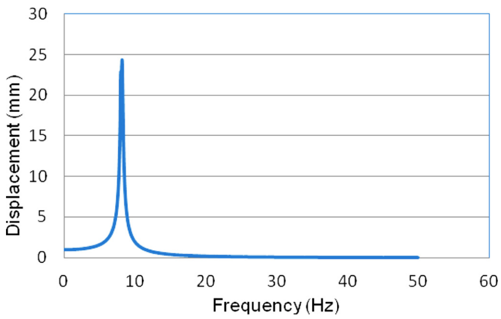

Fig. 6 Frequency response of the displacement of each mass when base excitations are in-phase

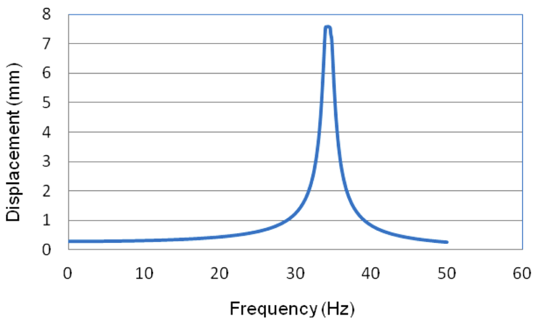

Fig. 7 Frequency response of the displacement of each mass when base excitations are out-of-phase

mass displacement for the adaptive multi-mode energy harvester is 7.6 mm at 33.9 Hz. The inertial force (F_{n2}) applied to each mass and the torque (M_{n2}) distribution along the beam are

$$F_{n2} = K_2 u_{n2} = \frac{3EI}{(0.105L)^2(L)} u_{n2} \tag{41}$$

$$M_{n2} = \begin{cases} 0.3F_{n2}x & 0 \le x \le 0.35L \\ 0.3F_{n2}x - F_{n2}(x - 0.35L) & 0.35L \le x \le 0.65L \\ -0.3F_{n2}(L - x) & 0.65L \le x \le L \end{cases} \tag{42}$$

Then the force factor at the second mode can be calculated from Eqs. (14) and (15).

$$\alpha_{n2} = 0.02625\frac{\gamma dLF_{n2}}{I} \tag{43}$$

5. Discussion

5.1 Comparison between single-mode and multi-mode energy harvesters under the first resonant frequency

Assuming harmonic excitation with the same amplitude is applied to the bases of both multi-mode and single mode energy harvesters and two designs have the same beam dimensions, the amplitude ratio between the force factors of a multi-mode energy harvester in Fig. 2 or 3 and a single-mode energy harvester under the first resonant frequency can be calculated from Eqs. (18), (19), (29), (36), and (38).

$$\frac{\hat{\alpha}_{1,m}}{\alpha_m} = 0.228\frac{\hat{\omega}_1^{\,2} m_1 \xi_n}{\omega_n^{\,2} m \xi_1} \tag{44}$$

Where $\hat{\alpha}_{1,m}$ and α_m are the amplitudes of the force factors of the multi-mode energy harvester under the first resonant frequency and the single-mode energy harvester, respectively. As the multi-mode energy harvester is analyzed under the first resonant frequency, ξ_n refers to the damping ratio in the first mode.

From Eq. (12), the ratio between the maximum harvested power is

$$\frac{P_{1,\max}}{P_{\max}} = \frac{\hat{\alpha}_{1,m}^{\,2}\hat{\omega}_1 Y_{1,m}^{\,2}}{\alpha_m^{\,2}\omega_n u_m^{\,2}} \tag{45}$$

Where $P_{1,\max}$ and $P_{\max}$ are the maximum power harvested by the multi-mode and single-mode energy harvesters under the first resonant frequency, $Y_{1,m}$ is the modal amplitude of the first mode for the multi-mode energy harvester, and u_m is the amplitude of the mass displacement at resonance for the single-mode energy harvester.

Based on Eqs. (9), (19), (32), (33), (43) and (44), the comparison between the multi-mode and single-mode energy harvesters, subject to the base harmonic motion at the first resonant frequencies, is shown in Table 2 for different mass ratios. For a fixed mass ratio (m_1/m), the maximum power ratio between the multi-mode and single-mode energy harvesters is affected by the ratio between damping ratios of the single-mode and multi-mode energy harvesters. If both designs have the same damping ratio, the multi-mode energy harvester can scavenge higher electrical power compared with the single-mode energy harvester. However, with a fixed design dimension, the multi-mode energy harvester requires much larger mass to achieve the same resonant frequency as that of the

Table 2 Comparison between the multi-mode and single-mode energy harvesters under the first resonant frequency

$m_1/m=m_2/m$	1	4	10
$\hat{\omega}_1/\omega_n$	3.1928	1.5964	1.0097
$\hat{\alpha}_{1,m}/\alpha_n$	$2.3242\frac{\xi_n}{\hat{\xi}_1}$	$2.3242\frac{\xi_n}{\hat{\xi}_1}$	$2.3242\frac{\xi_n}{\hat{\xi}_1}$
$Y_{1,m}/u_m$	$\frac{\xi_n}{\hat{\xi}_1}$	$\frac{\xi_n}{\hat{\xi}_1}$	$\frac{\xi_n}{\hat{\xi}_1}$
$P_{1,\max}/P_{\max}$	$17.2472\left(\frac{\xi_n}{\hat{\xi}_1}\right)^4$	$8.6236\left(\frac{\xi_n}{\hat{\xi}_1}\right)^4$	$5.4543\left(\frac{\xi_n}{\hat{\xi}_1}\right)^4$

cantilever-based energy harvester. No matter what masses both designs have, the ratio between the force factor amplitudes of two designs is only proportional to the ratio between damping ratios of the single-mode and multi-mode energy harvesters if other design parameters are same.

5.2 Comparison between the first two modes of the adaptive multi-mode energy harvester

The numerical results in section 4 are used for comparison between the first two modes of the adaptive multi-mode energy harvester. From Eqs. (39), (40), (41) and (43), the force factor amplitude ratio between the first and second modes can be calculated.

$$\frac{\alpha_{n1,m}}{\alpha_{n2,m}} = 0.78 \tag{46}$$

As the ratio between the maximum mass displacement from numerical simulation represents the ratio between the modal amplitudes in the first two modes, the ratio between maximum power harvested at the first two modes can be calculated from Eq. (12).

$$\frac{P_{1,\max}}{P_{2,\max}} = \frac{\alpha_{n1,m}^{2}\hat{\omega}_1 Y_{1,m}^{2}}{\alpha_{n2,m}^{2}\hat{\omega}_2 Y_{2,m}^{2}} = 1.49 \tag{47}$$

The maximum power harvested at the second vibration mode is about 67% of that harvested at the first vibration mode if the amplitudes of harmonic motions applied to the base at both frequencies are same.

6. Conclusions

Theoretical analysis is performed on a sample multi-mode energy harvester design with a simply supported beam and distributed mass and piezoelectric elements to investigate the feasibility of harvesting energy at two different resonant modes. The analysis shows that the second mode of the multi-mode design can not be excited if both supports experience the same harmonic motion. Based on the results, an adaptive multi-mode energy harvester concept is proposed. The adaptive multi-mode energy harvester adds an adaptive damper to one or both supports so that the motions of the two supports are synchronized at the first resonant frequency, but have a 180 degree phase shift at the second mode. The numerical simulation demonstrates that the adaptive multi-mode design can efficiently harvest energy at the first two resonant modes.

The energy harvesting capability of the multi-mode energy harvester is compared with that of the cantilever-based single-mode energy harvester. Results show that the multi-mode design has higher energy harvesting capacity compared with that of the single-mode energy harvester if both designs have similar damping ratios, even for an environment with a single vibration frequency.

As the energy harvesting capacity is related to the damping ratio, further work will concentrate on studying the damping characteristics of different harvester designs. In addition, design of adaptive dampers will be investigated to effectively adjust the phase shift between motions of two supports at the second resonant frequency for the adaptive multi-mode energy harvester. The design concept of a tuned mass damper traditionally used for vibration mitigation may be borrowed to create out-of-phase resonance at a desired frequency (Den Hartog 1947, Zuo 2009).

References

Anton, S.R. and Sodano, H.A. (2007), "A review of power harvesting using piezoelectric materials (2003-2006)", *Smart Mater.Struct*., **16**(3), R1-21.

Bach, U., Lupo, D., Comte, P., Moser, J.E.,Weissörtel, F., Salbeck, J., Spreitzer, H. and Grätzel, M. (1998), "Solid-state dyesensitized mesoporous TiO_2 solar cells with high photon-to-electron conversion efficiencies", *Nature*, **395**, 583-585.

Burton, T., Sharpe, D., Jenkins, N. and Bossanyi, E. (2001), *Wind energy handbook* , John Wiley & Sons.

Clough, R.W. and Penzien, J. (1993), *Dynamics of structures*, New York: McGraw-Hill.

Cullen, J.R., Teter, J.P., Wun-Fogle, M., Restorff, J.B. and Clark, A.E. (1997), "Magnetic and magnetoelastic studies of single crystal Tb06Dy04Zn at low temperatures", *IEEE T. Mag*., **33**(5), 3949-3951.

Den Hartog, J.P. (1947), *Mechanical vibration*, New York: McGraw-Hill.

El-hami, M., Glynne-Jones, P., White, N.M., Hill, M., Beeby, S., James, E., Brown, A.D. and Ross, J.N. (2001), "Design and fabrication of a new vibration-based electromechanical power generator",*Sensor. Actuat. A - PHYS*, **92**(1-3), 335-42.

Engel, T.G., Keawboonchuay, C. and Nunnally, W.C. (2000), "Energy conversion and high power pulse production using miniature piezoelectric compressors", *IEEE T. Plasma Sci*., **28**(5), 1338-1341.

Gao, R.X., Kazmer, D.O., Zhang, L., Theurer, C. and Cui, Y. (2004), "Self-powered sensing for mechanical system condition monitoring", *Proceedings of the SPIE - Smart Structures and Materials 2004: Sensors and Smart Structures,* Technologies for Civil, Mechanical and Aerospace Systems, **5391**, 321-330.

Glynne-Jones, P., Tudor, M.J., Beeby, S.P. and White, N.M. (2004), "An electromagnetic vibration-powered generator for intelligent sensor systems", Sensor. Actuat. *A - Phys*, **110**(1-3), 344-349.

James, E.P., Tudor, M.J., Beeby, S.P., Harris, N.R., Glynne-Jones, P., Ross, J.N. and White, N.M. (2004), "An investigation of self-powered systems for condition monitoring applications", *Sensor. Actuat. A - Phys*, **110**(1-3), 171-176.

Keawboonchuay, C. and Engel, T.G. (2003), "Electrical power generation characteristics of piezoelectric generator under quasi-static and dynamic stress conditions", *IEEE T. Ultrason. Ferr*., **50**(10), 1377-1382.

Lee, S., Youn, B.D. and Jung, B.C. (2009), "Robust segment-type energy harvester and its application to a wireless sensor", *Smart Mater. Struct*., **18**(9), 095021.

Lefeuvre, E., Badel, A., Richard, C. and Guyomar, D. (2005), "Piezoelectric energy harvesting device optimization by synchronous electric charge extraction", *J. Intell. Mater. Syst. Struct*., **16**(10), 865-876.

Leland, E.S., Lai, E.M. and Wright, P.K. (2004), "A self-powered wireless sensor for indoor environmental monitoring", *Proceedings of theWNCG 2004 Wireless Networking Symp*., Austin, TX, October 2004.

Leland, E.S. and Wright, P.K. (2006), "Resonance tuning of piezoelectric vibration energy scavenging generators using compressive axial preload", *Smart Mater. Struct*., **15**(5), 1413-1420.

Lesieutre, G.A., Ottman, G.K. and Hofmann, H.F. (2004), "Damping as a result of piezoelectric energy harvesting", *J. Sound Vib*., **269**(3-5), 991-1001.

Lysne, P.C. and Percival, C.M. (1975), "Electric energy generation by shock compression of ferroelectric ceramics: normal-mode response of PZT 95/5", *J. Appl. Phys*., **46**(4), 1519-1525.

MacNeil, D.D. and Sargent, E.H. (2006), "Solution-processed infrared photovoltaic devices", *Proceedings of the Design Automation Conference* (IEEE Cat. No. 06CH37797) .

Mitcheson, P.D., Green, T.C., Yeatman, E.M. and Holmes, A.S. (2004), "Architectures for vibration driven micropower generators", J. *Microelectrom.* S., **13**(3), 429-440.

Morris, D.J., Youngsman, J.M., Anderson, M.J. and Bahr, D.F. (2008), "A resonant frequency tunable, extensional mode piezoelectric vibration harvesting mechanism", *Smart Mater. Struct*., **17**(6), 065021.

Munteanu, I., Guiraud, J., Roye, D., Bacha, S. and Bratcu, A.I. (2006), "Sliding mode energy-reliability optimization of a variable speed wind power system", *Proceedings of the 2006 Int. Workshop on Variable Structure Systems*, Alghero, Italy.

Neugebauer, H., Brabec, C., Hummelen, J.C. and Sariciftci, N.S. (2000), "Stability and photodegradation mechanisms of conjugated polymer/fullerence plastic solar cells", *Solar Energy Mater.Solar Cells*, **61**(1), 35-42.

Ottman, G.K., Hofmann, H.F., Bhatt, A.C. and Lesieutre, G .A. (2002), "Adaptive piezoelectric energy harvesting circuit for wireless remote power supply", *IEEE T. Power Electr*., **17**(5) 669-676.

Paradiso, J.A. and Starner, T. (2005), "Energy scavenging for mobile and wireless electronics", *IEEE Pervas. Comput*., **4**(1) 18-27.

Qi, S., Shuttleworth, R., Oyadiji, S.O. and Wright, J. (2010), "Design of a multiresonant beam for broadband piezoelectric energy harvesting", *Smart Mater. Struct*., **19**(9), 094009.

Richard, C.D., Anderson, M.J., Bahr, D.F. and Richards, R.F. (2004), "Efficiency of energy conversion for devices containing a piezoelectric component", *J. Micromech. Microeng*., **14**(5), 717-721.

Roundy, S, Wright, P.K. and Rabaey, J. (2003)," A study of low level vibrations as a power source for wireless sensor nodes", *Comput. Commun*., **26**(11) 1131-1144.

Roundy, S. and Wright, P.K. (2004), "A piezoelectric vibration based generator for wireless electronics", *Smart Mater. Struct*., **13**(5), 1131-1142.

Roundy, S. (2005), "On the effectiveness of vibration-based energy harvesting", *J. Intell. Mater. Syst. Struct*., **16**(10), 809-823.

Roundy, S., Leland, E.S., Baker, J., Carleton, E., Reilly, E., Lai, E., Otis, B., Rabaey, J.M., Wright, P.K. and Sundararajan, V. (2005), "Improving power output for vibration-based energy scavengers", *IEEE Pervas. Comput*., **4**(1) 28-36.

Shahruz, S.M.(2006), "Design of mechanical band-pass filters with large frequency bands for energy scavenging", *Mechatronics*, **16**(9), 523-531.

Shahruz, S.M. (2008), "Design of mechanical band-pass filters for energy scavenging: multi-degree-offreedom models", *J. Vib. Control*., **14**(5), 753-768.

Shu, Y.C. and Lien, I.C. (2006), "Analysis of power output for piezoelectric energy harvesting systems," *Smart Mater.Struct*., **15**(6), 1499-1512.

Snyder, G.J., Lim J.R., Huang, C.K. and Fleurial, J.P. (2003), "Thermoelectric microdevice fabricated by a MEMS-like electrochemical process", *Nature Mater*., **2**(8), 528-531.

Sodano, H. A., Inman, D.J. and Park, G. (2004), "A review of power harvesting from vibration using piezoelectric materials", *Shock Vib*., **36**(3), 197-205.

Sterken, T., Fiorini, P., Baert, K., Puers, T. and Borghs, G. (2003), "An electret-based electrostatic m-generator", *Transducers*, **3**(2), 1291-1294.

Tiwari, R., Kim, K.J. and Kim, S. (2008), "Ionic polymer-metal composite as smart velocity sensors and energy harvesters", *Smart Struct. Syst*., **4**(5), 549-563.

Venkatasubramanian, R., Silivola, E., Colpitts, T. and O'Quinn, B. (2001), "Thin-film thermoelectric devices with high room-temperature figures of merit", *Nature*, **413**(6856), 597-602.

Xu, C.N., Akiyama, M., Sun, P. and Watanabe, T. (1997), "Novel approach to electrochromism in WO_3 thin film using piezoelectric ceramics as power supply", *Appl. Phys. Lett*., **70**(13), 1639-1640.

Yang, B., Lee, C., Xiang, W., Xie, J., He, J.H., Kotlanka, R.K., Low, S.P. and Feng, H. (2009), "Electromagnetic energy harvesting from vibrations of multiple frequencies", *J. Micromech Microeng*., **19**(3), 035001.

Yen, B.C. and Lang, J.H. (2006) "A variable-capacitance vibration-to-electric energy harvester", *IEEE T. Circ. Syst. Vid*., **53**(2), 288-295.

Yu, G., Gao, J., Hummelen, J.C., Wudl, F. and Heeger, A.J. (1995), "Polymer photovoltaic cells: enhanced efficiencies via a network of internal donor-acceptor heterojunctions", *Science,* **270**(5243), 1789-1791.

Yu, G. and Heeger, A.J. (1995), "Charge separation and photovoltaic conversion in polymer composites with internal donor/acceptor heterojunctions", *J. Appl. Phys*., **78**(7), 4510-4515.

Zhang, Y. and He, W. (2008), "Multi-mode piezoelectric energy harvesters for wireless sensor network based structural health monitoring", *Proceedings of the SPIE vol 6934 69340Z.*

Zhou, W., Penamalli, G.R. and Zuo, L. (2012), "An efficient vibration energy harvester with a multi-mode dynamic magnifier", *Smart Mater. Struct*., **21**(1), 015014.

Zuo, L. (2009), "Effective and robust vibration control using series multiple tuned-mass dampers", *J. Vib. Acoust*., **131**, 031003.

CC